# Synthesis and Crystal Structure of Nickel(II) Complexes of Macrobicyclic Ligands: Identification and Electron-transfer Reactions of the Corresponding Nickel(III) Complexes in Solution†

**Alexander McAuley,*[a] Denis G. Fortier,[b] Donal H. Macartney,[c] Todd W. Whitcombe[d] and Chao Xu[e]**

[a] *Department of Chemistry, University of Victoria, Victoria, British Columbia, V8W 2Y2, Canada*
[b] *MacMillan Bloedel Research Laboratories, Gilmore Way, Burnaby, British Columbia, Canada*
[c] *Department of Chemistry, Queen's University, Kingston, Ontario, Canada*
[d] *Department of Chemistry, Brandon University, Brandon, Manitoba, Canada*
[e] *Department of Chemistry, Lakehead University, Thunder Bay, Ontario, P7B 5E1, Canada*

The macrobicyclic complex $[NiL^1(ClO_4)]ClO_4$ ($L^1$ = 15-oxa-1,5,8,12-tetraazabicyclo[10.5.2]nonadecane) and the monocyclic precursor $[NiL^2(NCMe)][ClO_4]_2$, [$L^2$ = *N*,*N*′-bis(3-aminopropyl)-1-oxa-4,7-diazacyclononane] have been prepared and their crystal structures determined: $[NiL^1(ClO_4)]ClO_4$, space group $P2_1/n$, $a$ = 13.580(6), $b$ = 15.400(8), $c$ = 10.418(4) Å, β = 97.91(2)°, $Z$ = 4, $R$ = 0.067, $R'$ = 0.069; $[NiL^2(NCMe)][ClO_4]_2$, monoclinic, space group $Cc$, $a$ = 9.182(1), $b$ = 19.859(3), $c$ = 12.903(2) Å, β = 100.99(1)°, $Z$ = 4, $R$ = 0.063, $R'$ = 0.065. In each of these species the complexed cation is six-co-ordinate with the ether oxygen co-ordinated 'axially' at distances of 2.109(6) and 2.189(12) Å, respectively. However, the equatorial co-ordination is significantly different. In $[NiL^1(ClO_4)]^+$ the nickel atom is coplanar with the four nitrogen donors of the 14-membered macrocyclic ring. In $[NiL^2(NCMe)]^{2+}$ one pendant arm is axial (*trans* to the ether oxygen) with an acetonitrile molecule in the equatorial plane. Coplanarity of the equatorial donor set is not realized in this cation. The sixth position in $[NiL^1(ClO_4)]^+$ is occupied by a weakly bound perchlorate ion [Ni–O 2.373(7) Å]. The corresponding nickel(III) complexes may be generated by $Co^{3+}$(aq) oxidation in aqueous media or $NO^+$ in non-aqueous media. Electron spin resonance measurements are consistent with an octahedral $d^7$ ion with the spectra obtained being sensitive to the nature of the nuclei in the sixth site. The kinetics of reduction of the nickel(III) macrobicyclic ligand complex and its thiatetraaza and pentaaza analogues with two outer-sphere electron-transfer reagents has been studied. Rapid electron self-exchange rate constants have been evaluated for both the aqua and chloro species $[NiL(X)]^{n+}$ (X = $H_2O$, $n$ = 3; X = Cl, $n$ = 2), with a sensitivity to the nature of the axial ligands being observed.

A recent theme in the synthesis of macrocyclic metal complexes has been the extension of the ligand framework by use of pendant arms capable of both intra- and inter-molecular coordination.[1,2] Such species result in both mono- and polynuclear metal complexes with constrained donor environments but with the potential for specific site substitution.[3] Studies on nickel complexes with pendant-armed macrocycles have provided evidence for redox reactions with small molecules such as $CO_2$ and $O_2$.[4] A second area of interest is the co-ordination of metal ions by macrotricyclic ligands, wherein the possibility exists of complete encapsulation of the metal centre, resulting in complexes that are incapable of undergoing simple substitution reactions.[5] Such complexes are exemplified by the cryptate ligands, such as sepulchrate,[6] and the crown ether cryptands, such as 4,7,13,16,21,24-hexaoxa-1,10-diazabicyclo[8.8.8]hexacosane.[7] While the former ligands have been utilized extensively with transition metals to form a series of redox-active, substitution-inert co-ordination compounds, extensive formation of d-block element complexes with the polyether cryptands has not been realized. Rather, crown ether bicyclic ligands have been used extensively in the co-ordination of Group I and II metals.

More recently, ring conformations within complexed cations have been analysed for oxygen and other donors and the disposition of the metal ion considered in such co-ordination environments. Structural variations exhibited by transition-metal complexes of macrocyclic ligands have been examined by a number of authors.[8–10] However, most approaches have referred to octahedral co-ordination geometry. An alternate analysis of ring conformation has been developed by Ounsworth and Weiler[11] in which the structure of the macrocyclic complex is examined in terms of the internal dihedral angles observed. Boeyens and Dobson[8] employed a similar analytical procedure for various transition-metal complexes. Ounsworth and Weiler extend the methodology by plotting maps, in polar coordinates, of the torsional angles within the macrocycle as a function of bond number. This approach has been utilized by Gandour and Fyles[8] to characterize the symmetry elements present in hexadentate crown ether complexes, with the resulting simplification of the observed symmetries to six point groups.

The crystal structure of the nickel(II) complex ion of the pendant-armed macrocycle *N*,*N*′-bis(3-aminopropyl)-1-oxa-4,7-diazacyclononane, $[NiL^2(NCMe)]^{2+}$, is presented. Five-co-ordinate copper(II) complexes of this ligand have been used in the template synthesis of macrobicyclic ligands.[12,13] Although there are structural differences in the disposition of the pendant arms in the nickel(II) case, there is evidence for ligation of the axial ether oxygen. Crystallographic data are also

† *Supplementary data available:* see Instructions for Authors, *J. Chem. Soc., Dalton Trans.*, 1994, Issue 1, pp. xxiii–xxviii.
*Non-SI unit employed:* G = $10^{-4}$ T.

presented on two macrobicyclic complexes of nickel wherein, as a result of a cyclam ring (1,4,8,11-tetraazacyclotetradecane) formation, the ligand is constrained structurally. In such circumstances the geometry of the fused nine-membered ring facilitates co-ordination of the axial donor. Analysis of the ligand geometry using dihedral angles illustrates the structural invariance within the complexes under investigation and similarities with other facially co-ordinated macrocyclic systems. It is also of interest to examine the integrity in solution of species containing these five-co-ordinate ligands. The paramagnetic nature of the octahedral $d^8$ nickel(II) ion precludes NMR investigations owing, in some instances, to line broadening. However, oxidation to the corresponding nickel(III) complex ions generates the ESR-active $d^7$ ion. Displacement at the sixth (axial) site by halide and other ions may be examined by use of spin–nuclear coupling. There is no evidence for the formation of disubstituted nickel(III) ions. It is suggested that for the nickel-(II) and -(III) ions there is constancy of co-ordination geometry between the crystalline and solvated species.

Although the stabilization of nickel(III) by tetraaza macrocyclic ligands has now been recognized for more than two decades,[14–23] there have been relatively few studies of substitution reactions at this metal centre.[18,20,24] This is, in part, due to the kinetic instability of the high-valence complexes in aqueous media. In contrast, when the inner co-ordination sphere of the nickel is fully ligated [*e.g.* in the bis(triazacyclononane) complex[25,26]], species of greater kinetic robustness are formed such that they find use as outer-sphere electron-transfer reagents.[27] In attempting to overcome the problem of ready self-decomposition, we have prepared a series of macrobicyclic ligands where, by incorporation of derivatives of the nine-membered ring onto the tetraazamacrocyclic ring, a square-pyramidal donor set $N_4X$ (X = NH, S or O) is formed, leaving a single site for substitution in the octahedral ion.[12,13] The present paper describes the investigation of the outer-sphere electron-transfer reactions of the nickel(III) complexes of these fused macrobicyclic ligands.

## Experimental

The free macrocyclic compounds were prepared by demetallation of the copper complexes prepared previously.[12,13] **CAUTION**: Complexes involving metal perchlorates are potentially hazardous and subject to explosion. Extreme caution must be exercised in their use.

$[NiL^1(ClO_4)]ClO_4$.—The salt $Ni(ClO_4)_2\cdot 6H_2O$ (0.1 g, 0.27 mmol) was added to an ethanol solution (50 $cm^3$) of the macrocycle[12] $L^1$ (0.1 g, 0.37 mmol). The solution was refluxed for 2 h, during which time it changed from green to light yellow and a pale purple precipitate formed. After filtration, the precipitate was dissolved in water (10 $cm^3$) containing concentrated $HClO_4$ (1 $cm^3$). The solution was warmed until all of the precipitate had dissolved and subsequent slow cooling produced very fine purple crystals which were filtered off. Subsequent recrystallization from aqueous $NaClO_4$ yielded X-ray-quality crystals (Found: C, 31.45; H, 5.55; N, 10.40. Calc. for $C_{14}H_{30}Cl_2N_4NiO_9$: C, 31.85; H, 5.75; N, 10.60%).

$[NiL^3(N_3)]ClO_4$.—The free macrocycle[13] $L^3$ (100 mg, 0.37 mmol) was dissolved in ethanol (50 $cm^3$) and a solution of $Ni(ClO_4)_2\cdot 6H_2O$ (148 mg, 0.40 mmol) in ethanol (10 $cm^3$) added. The mixture was refluxed for 30 min during which it changed from green to pink. After cooling, the pink precipitate was filtered off, rinsed with ethanol, and air dried (Found: C, 32.25; H, 6.00; Cl, 14.05; N, 13.30. Calc. for $C_{14}H_{31}Cl_2N_5NiO_9$: C, 31.90; H, 5.90; Cl, 13.45; N, 13.30%). The azide complex was prepared by dissolution of the perchlorate salt in an aqueous solution containing $NaN_3$. The solid obtained on standing was redissolved in acetonitrile and X-ray-quality crystals formed by ether diffusion.

$[NiL^2(NCMe)][ClO_4]_2$.—Demetallation of the corresponding copper(II) complex[13] was achieved by reaction with $Na_2S$. The resulting macrocycle was extracted into chloroform and isolated as a viscous oil by rotary evaporation. Reaction with an equimolar aqueous solution of $Ni(ClO_4)_2\cdot 6H_2O$ resulted in the formation of a purple solution from which a solid perchlorate complex was derived. Dissolution of the precipitate in acetonitrile and ether diffusion resulted in the formation of X-ray-quality crystals.

All other materials were reagent grade unless otherwise indicated.

*Physical Measurements*.—Infrared spectra were obtained as KBr discs using a Perkin-Elmer 283 grating spectrometer, ESR specta on a Varian E6S spectrometer using the diphenylpicrylhydrazyl radical (dpph, $g = 2.0037$) as a reference standard and UV/VIS spectra using either a Cary 17 or a Perkin-Elmer Lambda 4B dual-beam spectrometer.

Electrochemical measurements were made using a Princeton Applied Research model 273 potentiostat/galvanostat, equipped with an IBM personal computer running the program HEADSTART.[28] The electrochemical cell was a standard configuration with platinum working and counter electrodes and either a saturated calomel or a Ag–AgCl reference electrode. In aqueous solutions the supporting electrolyte was either 1.0 mol $dm^{-3}$ $LiClO_4$ or 0.5 mol $dm^{-3}$ $Li_2SO_4$, while 0.1 mol $dm^{-3}$ $[NBu^n_4][PF_6]$ was used in acetonitrile. Spectroscopic grade acetonitrile was freshly distilled before use over calcium hydride under an inert atmosphere.

The stopped-flow and data-acquisition system utilized in obtaining the data for the substitution kinetics has been previously described.[29] An Applied Photophysics DX-17MV stopped flow spectrophotometer equipped with an Acorn microcomputer was used in studying the electron-transfer kinetics. In both cases, the nickel(III) solutions were prepared *in situ* by oxidation of the appropriate nickel(II) species using a stoichiometric deficiency of $Co^{3+}(aq)$ in 4.5 mol $dm^{-3}$ $HClO_4$. Ionic strength was maintained by the appropriate concentrations of $Li^+/HClO_4$, $Li^+/HNO_3$, and $Li^+/CF_3SO_3H$. In all cases, the ionic strength introduced by the addition of the cobalt(III) oxidant was minimal but accounted for. The reactions were monitored in the visible or ultraviolet region of the spectrum, under conditions where pseudo-first-order kinetics prevailed.

*Crystallography*.—The experimental parameters for both structures are presented in Table 1. The crystals were mounted in glass Lindemann tubes using epoxy resin. A preliminary unit cell was obtained, in each case, by using Weissenberg and precession photography. The $[NiL^1(ClO_4)]ClO_4$ crystal was transferred to a Picker four-circle diffractometer automated with a PDP 11/10 computer. The unit cell was refined using 17 pairs of reflections in the range 2θ 16–44°. The intensity measurements were obtained by scanning in the θ–2θ mode using 160 steps of 0.01° in 2θ, counting for 0.25 s per step. The background radiation was measured for 20 s before and after each scan. A set of three standard reflections preceded each batch of 50 measurements, with no statistically significant change in intensity observed during the data collection. An absorption correction was made using a locally modified version of an existing procedure.[30a] The $[NiL^2(NCMe)][ClO_4]_2$ crystal was transferred to an Enraf–Nonius CAD4 diffractometer. The unit cell was refined by using 25 pairs of reflections in the 2θ range 24–46°. The intensity measurements were obtained with a scan speed of 12, while intensity standards were measured every hour. No appreciable change occurred in the standards during the data collection. An absorption correction was made using EMPABS.[30b]

The direct-methods package of SHELX 76[31] provided the location of the nickel atom for $[NiL^3(N_3)]ClO_4$, while MULTAN[32] was utilized to solve the phase problem and locate the nickel atom in $[NiL^2(NCMe)][ClO_4]_2$. Subsequent least-

squares refinement was performed using SHELX for all structures. The atomic scattering factors were those included in the SHELX program together with the nickel *f* curve obtained from the usual source.[33] For both $[NiL^1(ClO_4)]ClO_4$ and $[NiL^2(NCMe)][ClO_4]_2$ all the atoms were refined anisotropically.

Crystal data were collected for $[NiL^3(N_3)]ClO_4$. However, the quality restricted the anisotropic atoms to nickel, chlorine and four oxygens of the asymmetric unit ($R' = 0.102$). Reference is made to some of the bond distances measured, which confirm the geometry and location of the axially disposed NH group in the nine-membered ring [Ni–N 2.19(1) Å].

Hydrogen atoms were neither located nor included in calculated positions in any of these structures.

Additional material available, including that for $[NiL^3(N_3)]ClO_4$, from the Cambridge Crystallographic Data Centre comprises thermal parameters and remaining bond lengths and angles.

## Results and Discussion

The synthetic route developed for the formation of the macrobicyclic ligands employs the template-assisted reaction of the pendant-armed complexes of $Cu^{II}$ to achieve ring closure. The synthesis and structure of the thia analogue $[NiL^4(ClO_4)]ClO_4$ have been presented previously, together with the corresponding copper species.[12,13] Although cyclam-ring formation has been achieved using a template reaction at $Ni^{II}$,[34] in the current case no successful ring closure was observed. This result may be due to the disposition of the pendant arms in the octahedral ion $[NiL^2]^{2+}$(solv) compared to the square-pyramidal geometry of the corresponding copper(II) species. The nomenclature used for these ligands labels separately the four atoms of the equatorial plane and the axial donor atom.

*Molecular Structure.*—The ORTEP[35] presentations for the structures of the two complexes investigated in this work are provided in Figs. 1 and 2 together with the atomic labelling schemes. The fractional atomic coordinates and selected bond lengths and angles are provided in Tables 2–4. The macrobicyclic ligand in the $[NiL^1(ClO_4)]^+$ and $[NiL^3(N_3)]^+$ cations may be viewed as the fusion of a nine-membered cyclononane ring with a 14-membered cyclotetradecane ring. The co-ordination geometry around the metal centre is six-co-ordinate in both cations, with the ligand occupying five sites. The 14-membered macrocyclic ligand may be described as adopting a *trans*-I configuration using the terminology of Bosnich *et al.*[36] In this configuration the hydrogen atoms and/or substituents are all located on the same side of the ligand framework. The average in-plane Ni–N bond lengths in $[NiL^1(ClO_4)]^+$ and $[NiL^3(N_3)]^+$ are 2.064(7) and 2.06(3) Å respectively, statistically identical to the value of 2.07(1) Å obtained for the $[NiL^4(ClO_4)]^+$ cation, reported previously.[13a] In all three cases the actual or observed bond lengths represent a compromise between the calculated M–N distance for cyclam in the *trans*-I configuration (2.01 Å)[37] and the ideal high-spin $Ni^{II}$–N bond length (2.10 Å).[38] These values may be contrasted with the average bond length of 2.09(4) Å obtained for the $[NiL^2(NCMe)]^{2+}$ cation, which is closer to the putative ideal length. The geometry of the latter cation, however, contrasts with that of the macrobicyclic complexes in that one of the pendant arms does not occupy an equatorial position rather an axial site, with the acetonitrile co-ordinated in the equatorial plane. This results in two different sets of Ni–N distances, with N(2) and N(4) at a mean distance of 2.13(1) Å and the remaining nitrogen atoms at 2.07(2) Å. While the latter distances are close to the values obtained for the macrobicyclic system, the former values are considerably longer (≈0.06 Å) illustrating the compression around the metal centre arising from the presence of the equatorial macrocyclic ring. An alternative approach to the consideration of the disposition of the atoms in the macrocyclic ligand is provided by the technique of dihedral mapping as outlined by Ounsworth and Weiler.[11] This procedure considers the relative position of the atoms around the macrocyclic ligand as a function of the internal torsion angles. Polar coordinate plots of the angle as a function of the bond position provide a ready analysis of the symmetry of the complexes and similarities between related structures.

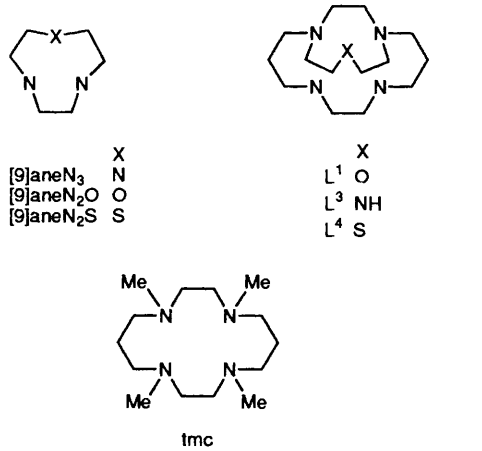


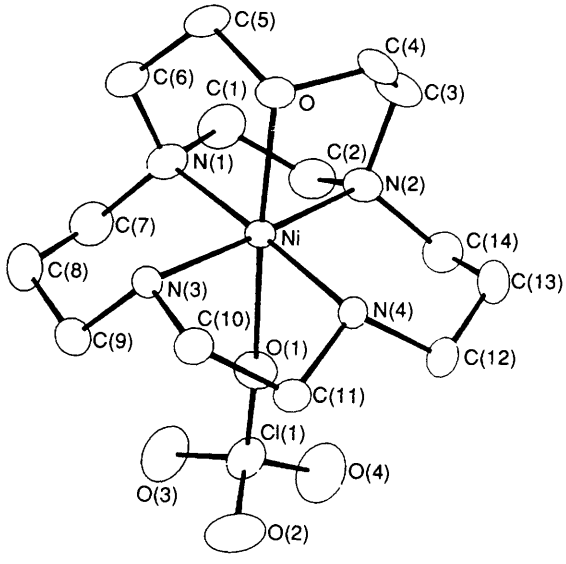


**Fig. 1** An ORTEP diagram of the $[NiL^1(ClO_4)]^+$ cation with 25% thermal ellipsoids

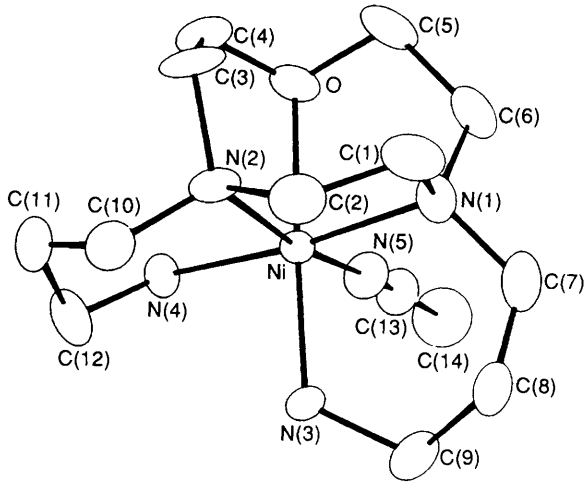


**Fig. 2** An ORTEP diagram of the $[NiL^2(NCMe)]^{2+}$ cation with 25% thermal ellipsoids

**Table 1** Experimental crystallographic parameters*

| | $[NiL^1(ClO_4)]ClO_4$ | $[NiL^2(NCMe)][ClO_4]_2$ |
|---|---|---|
| Formula | $C_{14}H_{30}Cl_2N_4NiO_9$ | $C_{14}H_{31}Cl_2N_5NiO_9$ |
| $M$ | 528 | 543.0 |
| Space group | $P2_1/n$ (no. 14) | $Cc$ (no. 9) |
| $a$/Å | 13.580(6) | 9.182(1) |
| $b$/Å | 15.400(8) | 19.859(3) |
| $c$/Å | 10.418(4) | 12.903(2) |
| β/° | 97.91(2) | 100.99(1) |
| $U$/Å$^3$ | 2158 | 2309.7 |
| $D_c$/g cm$^{-3}$ | 1.625 | 1.557 |
| $D_m$/g cm$^{-3}$ | 1.612 | 1.557 |
| Crystal size/mm | 0.12 × 0.81 × 0.16 | 0.84 × 0.20 × 0.28 |
| Total reflections | 2814 | 1483 |
| Observed reflections [$I > n\sigma(I)$] | 2125 ($n = 2$) | 1445 ($n = 1$) |
| No. parameters | 271 | 278 |
| Residual electron density/e Å$^{-3}$ | 0.60 | 0.76 |
| Maximum final shift/e.s.d. | 0.057 | 0.074 |
| $R,R'$ | 0.067, 0.069 | 0.063, 0.065 |

Details in common: $Z = 4$; Mo-Kα radiation (λ 0.710 69 Å); 2θ range 0.1–45°; $R = \Sigma(|F_o| - |F_c|)/\Sigma|F_o|$, $R' = [\Sigma(|F_o| - |F_c|)^2/\Sigma w(|F_o|)^2]^{\frac{1}{2}}$, $w = 0.001$.

**Table 2** Fractional coordinates (× 10$^4$ except Ni, × 10$^5$) for $[NiL^1(ClO_4)]ClO_4$

| Atom | $X/a$ | $Y/b$ | $Z/c$ |
|---|---|---|---|
| Ni | 56 623(7) | 25 595(6) | 22 382(10) |
| Cl(1) | 8 482(2) | 2 835(2) | 2 586(2) |
| Cl(2) | 2 876(2) | 4 801(1) | 1 946(3) |
| O | 4 140(4) | 2 281(4) | 2 216(6) |
| O(1) | 7 423(5) | 2 653(4) | 2 546(7) |
| O(2) | 8 603(7) | 3 354(6) | 1 482(8) |
| O(3) | 8 791(6) | 3 342(6) | 3 699(8) |
| O(4) | 9 010(7) | 2 063(6) | 2 578(9) |
| O(5) | 2 340(5) | 5 398(4) | 1 082(7) |
| O(6) | 3 242(5) | 4 115(5) | 1 250(8) |
| O(7) | 3 737(7) | 5 220(6) | 2 590(9) |
| O(8) | 2 280(9) | 4 522(7) | 2 789(12) |
| N(1) | 5 552(6) | 2 835(6) | 4 149(8) |
| N(2) | 5 828(5) | 1 273(5) | 2 826(8) |
| N(3) | 5 483(5) | 3 847(4) | 1 719(7) |
| N(4) | 5 761(5) | 2 342(4) | 312(6) |
| C(1) | 5 767(9) | 2 005(8) | 4 945(10) |
| C(2) | 6 318(8) | 1 347(7) | 4 176(10) |
| C(3) | 4 833(7) | 835(6) | 2 787(11) |
| C(4) | 4 024(7) | 1 362(6) | 1 871(10) |
| C(5) | 3 762(7) | 2 495(7) | 3 437(10) |
| C(6) | 4 500(7) | 3 131(7) | 4 169(10) |
| C(7) | 6 273(8) | 3 541(8) | 4 654(10) |
| C(8) | 6 117(8) | 4 422(7) | 3 900(12) |
| C(9) | 6 242(7) | 4 420(6) | 2 449(11) |
| C(10) | 5 488(7) | 3 890(5) | 264(9) |
| C(11) | 5 121(7) | 3 171(5) | −200(9) |
| C(12) | 6 401(7) | 1 614(6) | −55(10) |
| C(13) | 6 175(8) | 772(6) | 628(12) |
| C(14) | 6 503(8) | 748(6) | 2 067(12) |

Estimated standard deviations are given in parentheses.

**Table 3** Fractional coordinates (× 10$^4$ except Ni and Cl, × 10$^5$) for $[NiL^2(NCMe)][ClO_4]_2$

| Atom | $X/a$ | $Y/b$ | $Z/c$ |
|---|---|---|---|
| Ni | 56 810(7) | 17 878(6) | 34 710(7) |
| Cl(1) | 63 875(48) | 16 061(18) | 80 266(32) |
| Cl(2) | 7 889(50) | 5 557(26) | 11 718(41) |
| O | 7 894(12) | 1 690(6) | 4 400(11) |
| O(1) | 6 968(19) | 2 128(7) | 8 736(11) |
| O(2) | 5 160(30) | 1 343(12) | 8 243(28) |
| O(3) | 7 422(27) | 1 150(11) | 7 806(27) |
| O(4) | 6 059(39) | 1 927(16) | 7 093(15) |
| O(5) | 2 212(16) | 590(10) | 997(15) |
| O(6) | 111(25) | 1 148(13) | 678(15) |
| O(7) | 890(18) | 665(8) | 2 304(12) |
| O(8) | 55(32) | 53(14) | 925(25) |
| N(1) | 6 902(15) | 1 603(7) | 2 271(10) |
| N(2) | 5 723(16) | 729(5) | 3 364(9) |
| N(3) | 3 638(14) | 1 844(5) | 2 420(10) |
| N(4) | 4 659(14) | 1 966(7) | 4 745(10) |
| N(5) | 5 990(17) | 2 828(7) | 3 381(13) |
| C(1) | 6 982(21) | 844(11) | 2 133(15) |
| C(2) | 5 814(20) | 468(7) | 2 594(14) |
| C(3) | 7 124(18) | 524(7) | 4 427(14) |
| C(4) | 7 854(18) | 1 135(8) | 5 089(13) |
| C(5) | 9 043(17) | 1 633(11) | 3 776(15) |
| C(6) | 8 395(19) | 1 914(11) | 2 675(15) |
| C(7) | 6 333(25) | 1 936(11) | 1 235(15) |
| C(8) | 4 725(22) | 1 753(10) | 762(12) |
| C(9) | 3 562(21) | 2 161(9) | 1 335(12) |
| C(10) | 4 381(19) | 455(9) | 4 025(15) |
| C(11) | 4 125(23) | 759(9) | 5 054(16) |
| C(12) | 3 488(21) | 1 465(11) | 4 922(16) |
| C(13) | 6 097(18) | 3 381(8) | 3 366(14) |
| C(14) | 6 190(32) | 4 116(10) | 3 249(26) |

Estimated standard deviations are given in parentheses.

Application of this technique is illustrated in Fig. 3 where the dihedral map of the nine-membered rings within the bicyclic ligands is plotted. (The corresponding data for the fourteen-membered rings have been deposited.) For comparison, the dihedral maps derived from the crystallographic data[39-41] for the corresponding tridentate [9]aneN$_2$X (X = NH, O or S) complexes of nickel(II) have been incorporated into the plot. [Similarly, monocyclic maps for the *N*-methylated cyclam complexes of nickel(II) have been included in the plot of the 14-membered ring.[42,43]] It is apparent that the nine-membered rings are isostructural both with regard to the mono- and bicyclic analogues and the inclusion of the various axial donor atoms. The geometry of the ring is invariant in going from oxygen and nitrogen to sulfur. This result might have been anticipated since the ligands do not exhibit any significant structural variations except in the C–N, C–O, or C–S bond lengths, but the dihedral mapping demonstrates that changes in these bond lengths are compensated in the M–X bond-length variation and that the ligand adopts a constant geometry. Analysis of the dihedral map of the 14-membered ring illustrates the interesting feature that the chelating rings in the macrocycles adopt a *trans*-I geometry. However, there are structural differences between the geometry adopted by the $[Ni(tmc)]^{2+}$ species (tmc = 1,4,8,11-tetramethyl-1,4,8,11-tetraazacyclotetradecane) and the macrobicyclic complexes. Indeed, the [Ni-

**Table 4** Selected bond lengths (Å) and angles (°)

| | | | |
|---|---|---|---|
| (*a*) $[NiL^1(ClO_4)]ClO_4$ | | | |
| O–Ni | 2.109(6) | O(1)–Ni | 2.373(7) |
| N(1)–Ni | 2.061(8) | N(2)–Ni | 2.077(7) |
| N(3)–Ni | 2.061(6) | N(4)–Ni | 2.057(7) |
| O(1)–Ni–O | 169.2(2) | N(3)–Ni–N(1) | 92.0(3) |
| N(1)–Ni–O | 81.4(3) | N(3)–Ni–N(2) | 178.0(3) |
| N(1)–Ni–O(1) | 93.6(3) | N(4)–Ni–O | 98.7(2) |
| N(2)–Ni–O | 82.9(2) | N(4)–Ni–O(1) | 86.7(3) |
| N(2)–Ni–O(1) | 87.2(3) | N(4)–Ni–N(1) | 177.4(3) |
| N(2)–Ni–N(1) | 86.0(3) | N(4)–Ni–N(2) | 96.5(3) |
| N(3)–Ni–O | 96.4(2) | N(4)–Ni–N(3) | 85.5(3) |
| N(3)–Ni–O(1) | 93.3(3) | | |
| (*b*) $[NiL^2(NCMe)][ClO_4]_2$ | | | |
| O–Ni | 2.189(12) | N(1)–Ni | 2.051(12) |
| N(2)–Ni | 2.127(11) | N(3)–Ni | 2.065(12) |
| N(4)–Ni | 2.135(12) | N(5)–Ni | 2.087(13) |
| N(1)–Ni–O | 80.1(5) | N(4)–Ni–N(2) | 92.4(5) |
| N(2)–Ni–O | 80.6(5) | N(4)–Ni–N(3) | 90.3(5) |
| N(2)–Ni–N(1) | 86.2(5) | N(5)–Ni–O | 89.2(5) |
| N(3)–Ni–O | 176.5(5) | N(5)–Ni–N(1) | 93.8(5) |
| N(3)–Ni–N(1) | 96.7(5) | N(5)–Ni–N(2) | 169.6(7) |
| N(3)–Ni–N(2) | 97.8(5) | N(5)–Ni–N(3) | 92.5(6) |
| N(4)–Ni–O | 92.9(5) | N(5)–Ni–N(4) | 86.4(5) |
| N(4)–Ni–N(1) | 173.0(6) | | |

Estimated standard deviations are given in parentheses.

**Table 5** Calculated mean planes

| Atom | *X* | *Y* | *Z* | *P* | e.s.d.(*P*) |
|---|---|---|---|---|---|
| (*a*) $[NiL^1(ClO_4)]ClO_4$ | | | | | |
| N(1) | 6.9451 | 4.3656 | 4.2810 | −0.0033 | 0.0082 |
| N(2) | 7.5100 | 1.9597 | 2.9160 | 0.0025 | 0.0073 |
| N(3) | 7.1990 | 5.9241 | 1.7733 | 0.0022 | 0.0067 |
| N(4) | 7.7783 | 3.6071 | 0.3219 | −0.0019 | 0.0068 |
| Sum of *P*(I) −0.0005 | | | | | |
| Ni | 7.3685 | 3.9415 | 2.3096 | −0.0049 | 0.0010 |
| O | 5.3038 | 3.5127 | 2.2864 | 2.0677 | 0.0058 |
| O(1) | 9.7153 | 4.0862 | 2.6268 | −2.3692 | 0.0068 |
| (*b*) $[NiL^2(NCMe)][ClO_4]_2$ | | | | | |
| N(1) | 5.7785 | 3.1830 | 2.8770 | 0.0303 | 0.0132 |
| N(2) | 4.3537 | 1.4471 | 4.6413 | −0.0261 | 0.0136 |
| N(4) | 3.1103 | 3.9039 | 6.0106 | 0.0280 | 0.0130 |
| N(5) | 4.6681 | 5.6159 | 4.2825 | −0.0403 | 0.0165 |
| Sum of *P*(I) −0.0081 | | | | | |
| Ni | 4.3758 | 3.5504 | 4.3281 | 0.1564 | 0.0000 |
| O | 6.1656 | 3.3572 | 5.5733 | −2.0132 | 0.0124 |
| N(3) | 2.7451 | 3.6620 | 3.0653 | 2.2164 | 0.0128 |

*P* represents the extent of deviation from planarity.

$(N_4X)]^{2+}$ compounds are isostructural with $[Zn(tmc)]^{2+}$.[44] An alternate designation of the two sets of compounds is presented as [3434] and [3344],[8] respectively. Further analysis of macrocyclic ligands utilizing this schematic presentation will provide a better understanding and basis for comparison of the structural features demonstrated in these complexes.

Owing to the co-ordination of the anion in both macrobicyclic complexes, the geometry at the metal centre is pseudo-octahedral, which is again a feature consistent with the dihedral maps obtained. In the $[NiL^1(ClO_4)]^+$ cation the nickel atom lies in the plane described by the four nitrogen atoms with a perpendicular distance to the plane of 0.005 Å (Table 5). {In the $[NiL^3(N_3)]^+$ cation the four nitrogens of the fourteen-membered ring do not describe a perfect plane with deviations of about 0.04 Å from ideality, but the nickel, within these tolerances, is situated in the plane with a perpendicular distance of 0.01 Å.} In both cases, these results contrast with those for the $[NiL^4(ClO_4)]^+$ complex where the Ni is located 0.111 Å above the plane, towards the apical sulfur atom.[13a] These results are at variance with those predicted by Hancock and co-workers[45] for the *trans*-I configuration of cyclam where the nickel atom was calculated to reside 0.06 Å above the $N_4$ plane. The constraint of an axial donor, the octahedral co-ordination geometry, and the strength of the donor–metal bond all exert some influence on the disposition of the metal centre with regard to the macrobicyclic ligand. While the axial Ni–N bond lengths in the $[NiL^3(N_3)]^+$ are statistically equivalent [2.15(3) *vs.* 2.18(3) Å], the same is not true in the $[NiL^1(ClO_4)]^+$ cation. The Ni–O distance to the ether oxygen is 2.109(6) Å and to the $ClO_4^-$ oxygen is 2.373(7) Å. The difference in these bond lengths is a reflection of the weak binding of perchlorate anions in metal complexes although the nickel–perchlorate bond length is considerably shorter than that observed in the corresponding $[NiL^4(ClO_4)]^+$ cation [2.563(2) Å].[13a] Comparative distances for the nickel–ether bond are not readily available as there are so few data for such interactions. The $[NiL^2(NCMe)]^{2+}$ cation exhibits a similar interaction in which a slightly longer Ni–O bond is realized

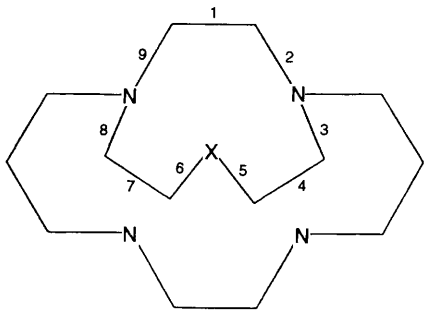


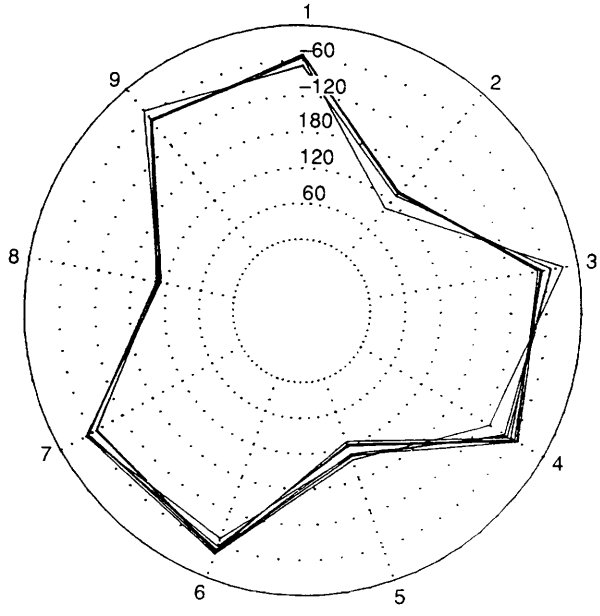


**Fig. 3** Dihedral map for nine-membered rings demonstrating constancy of geometry between $[Ni(N_4X)]^{2+}$ complexes and other facially co-ordinated cyclononane ligands

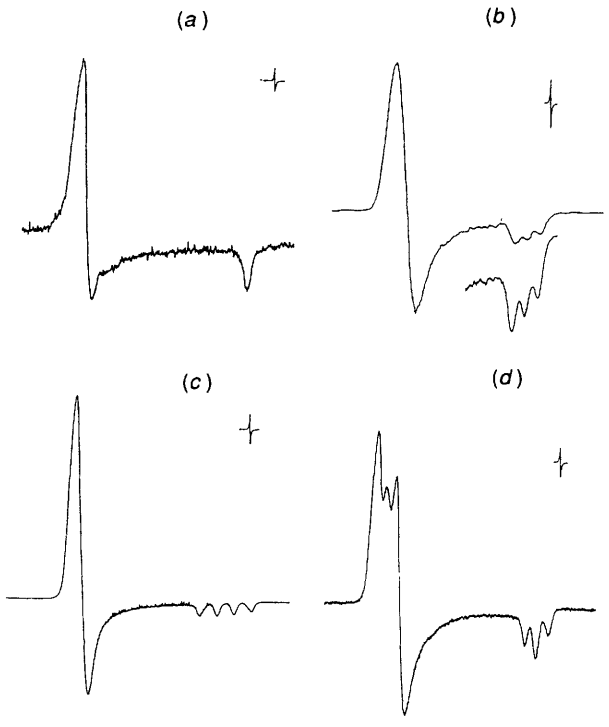


**Fig. 4** The ESR spectra in frozen matrix (77 K) of (*a*) $[NiL^1(OH_2)]^{3+}$ in water, (*b*) $[NiL^3(OH_2)]^{3+}$ in water, (*c*) $[NiL^1(Cl)]^{2+}$ in acetonitrile, and (*d*) $[NiL^1(NO)]^{3+}$ in $MeNO_2$

[2.19(1) Å]. However, the monocyclic cation is not ideally octahedral, with a marked deviation in the location of the two tertiary nitrogens from the equatorial plane of the nickel. The displacement at these positions not only lowers the co-ordination site symmetry but also facilitates elongation of the axial bonding interaction. Two similar complexes have been reported containing axial linkages to ether oxygen atoms. These are both variations of a 15-membered macrocyclic ligand containing an $N_2S_2O$ donor set.[46] In the 1-oxa-4,13-dithia-7,10-diazacyclopentadecane complex the ether Ni–O distance is 2.243(5) Å while for 1-oxa-7,10-dithia-4,13-diazacyclopentadecane complex the corresponding distance is 2.069(2) Å. By way of comparison, the mean metal–nitrogen distances in these complexes are 2.060 and 2.064 Å, respectively, while the mean sulfur distances are 2.410 and 2.416 Å. The consistency of these bond lengths and the variation in the nickel–ether distance suggests that the Ni–O interaction is not strongly defined and, together with the distances presented above, indicates a relatively flexible but persistent mode of co-ordination in these complexes.

*ESR Spectroscopy*.—The nickel(III) complexes of the macrobicyclic ligands are ESR active, yielding spectra characteristic of a low-spin $d^7$ ion in a distorted-octahedral environment of axial symmetry.[18,23,47,48] Oxidation of the $[NiL^1(H_2O)]^{2+}$ cation in acidic perchlorate media by $Co^{3+}(aq)$ yields a species with $g_\perp = 2.028$ and $g_\parallel = 2.200$ [Fig. 4(*a*)] where there is no evidence of hyperfine interaction as expected owing to the presence of only oxygen donors at the axial sites. These values may be compared with the parameters obtained for $[Ni(cyclam)(OH_2)_2]^{3+}$ under the same conditions ($g_\perp = 2.033$, $g_\parallel = 2.219$). This suggests that not only is the ether oxygen bound to the $Ni^{III}$ but it resembles spectroscopically the oxygen atom of a water molecule. The corresponding spectrum for the $[NiL^3(OH_2)]^{3+}$(solv) cation [Fig. 4(*b*)] has $g_\perp = 2.027$ and $g_\parallel = 2.173$ with $A_\parallel = 22$ G. The magnitude of the axial coupling constant is consistent with that observed in $[Ni(cyclam)(solv)_2]^{3+}$ complexes {$\approx 26$ G for $[Ni^{III}(cyclam)]^{3+}$ in acetonitrile}.[24] The net result is that nickel(III) complexes of the fused macrocyclic ligand resemble a $Ni(cyclam)^{3+}$ moiety with axial ligands comparable to simple solvent molecules. The difference is that, in the present case, there is no mechanism for a dissociation of the donor atoms incorporated in the fused macrocyclic ligand. Thus, solvent-exchange and anation reactions are limited to one site in the macrobicyclic nickel(III) species. Upon addition of chloride to the $[NiL^1]^{3+}$(solv) cation the spectrum observed was consistent with a single halide co-ordinated in the axial site ($g_\parallel = 2.033$, $A_\parallel = 29$ G; $g_\perp = 2.192$) [Fig. 4(*c*)]. An identical spectrum is obtained in acetonitrile (using $NO^+$ as oxidant). The formation of a monofluoro complex ion is confirmed in aqueous media by the coupling observed for both the parallel and perpendicular signals ($g_\parallel = 2.027$, $A_\parallel = 212$ G; $g_\perp = 2.189$, $A_\perp = 71$ G). These values are consistent with those reported previously for other nickel(III) macrocyclic complexes.[18,24,48] Of interest is the identification of a nitrogen-bonded nitrosyl complex in the reaction of $NOBF_4$ with $[NiL^1(solv)]^{2+}$ in $MeNO_2$, a non-co-ordinating solvent. Splitting of the $g_\parallel$ and $g_\perp$ features if consistent with equilibration of the $NO^\bullet$ radical and with extensive electron delocalization in the complex [Fig. 4(*d*)]. Despite attempts at forcing the co-ordination of a second axial anion by the addition of a large excess of halide ion and heating, no evidence for displacement of the bound ether oxygen was obtained in either room-temperature or 77 K spectra. Addition of chloride to the $[NiL^3(solv)]^{3+}$ cation results in the formation of the monochloro complex with a similar observed ESR spectrum [$g_\parallel = 2.024$, $A_\parallel(Cl,N) = 22$ G, $g_\perp = 2.160$]. The axial coupling parameter is the observed peak separation which is a composite of the axial coupling due to both the nitrogen and chlorine nuclei. Similar results were obtained in fluoride media where the axial feature is rendered as a doublet of triplets [$g_\parallel = 2.027$, $A_\parallel(F) = 198, 19$ G; $g_\perp = 2.189$, $A_\perp = 60$ G]. The decrease in magnitude of the coupling constants and $g$ values is consistent with a slightly greater degree of electron delocalization onto the apical nitrogen in these complexes, reflecting the relative 'hard/soft' nature of the secondary amine and ether oxygen atoms. In order further to examine the strength of the Ni–O bond in macrocyclic ether complexes, ESR spectra were obtained for the structurally analogous cation, $[Ni([9]aneN_2O)_2]^{3+}$ ([9]aneN$_2$O = 1-oxa-4,7-diazacyclononane) where the geometry is such that the oxygen atoms are located in *trans* positions. Oxidation of the complex by either $NOBF_4$ in $MeNO_2$ or $Co^{3+}(aq)$ and subsequent addition of a large molar excess of fluoride ion resulted in no discernible changes in the spectra. This is consistent with no ligation of $F^-$ and maintenance of the octahedral co-ordination of the macrocycle in the oxidized ion. Comparison with the results obtained for $[NiL^1(X)]^{2+}$ reinforces the view that only monosubstitution occurs in the latter species.

*Electrochemistry*.—Cyclic voltammetry of the macrobicyclic nickel complexes in 1 $dm^{-3}$ $HClO_4$ displayed reversible waves, independent of scan rate, with potentials of 1.123 and 0.976 V (*vs.* normal hydrogen electrode, NHE) for the $[NiL^1]^{3+/2+}$ and $[NiL^3]^{3+/2+}$ couples, respectively. In the former case this is significantly higher than the corresponding redox couple for $[Ni(cyclam)]^{3+/2+}$ (0.99 V)[16,24] and may reflect either the strain in the oxidant or a greater thermodynamic stability for the nickel(II) ion. The latter value is almost identical to that obtained for $[Ni([9]aneN_3)_2]^{3+/2+}$ and is similar to the redox potential obtained for the hexaaza macrocyclic complexes of nickel.[26,39,49,50] Intermediate between these two results is the value of 1.07$_6$ V (*vs.* NHE) (Table 6) obtained for $[NiL^4]^{3+/2+}$ under identical conditions.[14a]

The crystallographic analysis suggests that the differences in these values are not dependent upon structural variations in the cationic complexes. Such differences are then attributable to changes in the electronic interactions within the metal complexes, reflecting the nature of the axially co-ordinated ligand. However, corresponding variations in the spectroscopic parameters for these complexes are not exhibited. The

**Table 6** Rate constants and activation parameters for the reduction of $[Ni(N_4X)(OH_2)]^{3+}$ and $[Ni(N_4X)Cl]^{2+}$ by $[Ni([9]aneN_3)_2]^{2+}$. Calculated self-exchange rate constants for the $[Ni(N_4X)(OH_2)]^{3+/2+}$ and $[Ni(N_4X)Cl]^{2+/+}$ couples

| Parameter | $[NiL^3]^{3+}$ | $[NiL^4]^{3+}$ | $[NiL^1]^{3+}$ |
|---|---|---|---|
| (*a*) Aqua complex | | | |
| $10^{-4}\ k_1$/dm$^3$ mol$^{-1}$ s$^{-1}$ | 3.20 ± 1.0 | 34.7 ± 0.05 | 64.0 ± 1.0 |
| $\Delta H_1^{\ddagger}$/kJ mol$^{-1}$ | 28.2 ± 1.5 | 22.2 ± 0.3 | 27.3 ± 1.4 |
| $\Delta S_1^{\ddagger}$/J K$^{-1}$ mol$^{-1}$ | −64 ± 4 | −64 ± 1 | −42 ± 4 |
| (*b*) Chloro complex | | | |
| $10^{-4}\ k_2$/dm$^3$ mol$^{-1}$ s$^{-1}$ | 0.65 ± 0.06 | 6.1 ± 0.4 | 5.7 ± 0.1 |
| $\Delta H_2^{\ddagger}$/kJ mol$^{-1}$ | 32.0 ± 1.2 | 23.5 ± 0.6 | 24.8 ± 1.2 |
| $\Delta S_2^{\ddagger}$/J K$^{-1}$ mol$^{-1}$ | −62 ± 4 | −73 ± 2 | −71 ± 4 |
| $K_{Cl}$ | 12 ± 1[a] | 25 ± 2[a] | ≈100[b] |
| $E_{\frac{1}{2}}^{\circ}(ClO_4^-)$[c] | $0.97_6$ | $1.07_6$ | $1.12_3$ |
| $E_{\frac{1}{2}}^{\circ}(Cl^-)$[c] | $0.92_5$ | $1.02_2$ | $1.04_0$ |
| $10^{-5}\ k_{11}(H_2O)$/dm$^3$ mol$^{-1}$ s$^{-1}$ | 0.56 | 1.6 | 1.0 |
| $10^{-4}\ k_{11}(Cl^-)$/dm$^3$ mol$^{-1}$ s$^{-1}$ | 1.4 | 2.8 | 1.3 |

[a] 25.0 °C; $I$ = 1.00 mol dm$^{-3}$. [b] 9.0 °C; $I$ = 1.00 mol dm$^{-3}$. [c] In V *vs.* NHE.

electrochemical potential of all three complexes is sensitive to the presence of other anions. Measurement of the redox potential for the $[NiL]^{3+/2+}$ couples in 1.0 mol dm$^{-3}$ HCl results in a decrease in the observed values (Table 6) to 1.040, 0.925 and 1.022 V for $[NiL^1(Cl)]^{2+/+}$, $[NiL^3(Cl)]^{2+/+}$, and $[NiL^4(Cl)]^{2+/+}$, respectively. The differences in the redox potentials may be used to calculate[51] the ratio of the complexation constants for the nickel(III) and nickel(II) chloride species, with values of 25.3, 7.3 and 8.2 obtained. Complexation constants for the $[NiL(Cl)]^{2+}$ species have been derived from the kinetic measurements (see below) with values of ≈100 (9°C), 12 and 25 dm$^{-3}$ mol$^{-1}$ respectively. Assuming only a small temperature variation for the constants, and if the above constants represent the ratios of the equilibrium constants for the oxidised and reduced forms of the metal complexes, $K_{ox}/K_{red}$, values in the range 2–4 for $K_{red}$ are derived. These ratios obtained are consistent with those obtained previously for other nickel macrocyclic complexes.[24,52]

*Spectrophotometric Titration.*—The complex $[NiL^1(ClO_4)]ClO_4$ in water yields a solution of considerable stability as might be anticipated for a macrocyclic metal complex. The spectroscopic features are characteristic of an octahedral nickel(II) ion with four absorptions observable in the UV/VIS region ($\varepsilon_{222} = 2.42 \times 10^3$, $\varepsilon_{337} = 17$, $\varepsilon_{515} = 10$, and $\varepsilon_{681} = 5$ dm$^3$ mol$^{-1}$ cm$^{-1}$). Some decomposition of the complex is observed in strongly acid solutions (>4 mol dm$^{-3}$) but this is sufficiently slow that it does not impede any kinetic investigation. Titration of the nickel(II) complex with $Co^{3+}$(aq) in 2.0 mol dm$^{-3}$ $HClO_4$ resulted in absorbance changes consistent with the stoichiometry required for a one-electron oxidative titration to the nickel(III) complex. The UV/VIS spectrum was typical of octahedral nickel(III) macrocyclic compounds [$\varepsilon_{261} = (6.6 \pm 0.2) \times 10^3$, $\varepsilon_{326}$(sh) = $(4.9 \pm 0.4) \times 10^3$, $\varepsilon_{374}$(sh) = $(5.3 \pm 0.3) \times 10^3$, and $\varepsilon_{634} = 37 \pm 2$ dm$^3$ mol$^{-1}$ cm$^{-1}$]. The absorption coefficients were obtained by extrapolation of kinetic plots to zero time, owing to decomposition of the nickel(III) ion during the titration.

*Electron-Transfer Kinetics.*—The kinetics of the electron-transfer reactions between the $[Ni(N_4X)]^{3+}$ cations and the outer-sphere reagent $[Ni([9]aneN_3)_2]^{2+}$ [equation (1)] was investigated in acidic perchlorate media in the absence and presence of chloride ions. The rate constants were measured under pseudo-first-order conditions with an excess of the reductant $[Ni([9]aneN_3)_2]^{2+}$. The $[Ni(N_4X)(OH_2)]^{3+}$ species were generated immediately prior to reaction by oxidation with a slight stoichiometric deficiency of $Co^{3+}$(aq). The observed first-order rate constants displayed a linear dependence on the concentration of $[Ni([9]aneN_3)_2]^{2+}$ [equation (2)], where

$$[Ni(N_4X)(OH_2)]^{3+} + [Ni([9]aneN_3)_2]^{2+} \xrightarrow{k_1} [Ni(N_4X)(OH_2)]^{2+} + [Ni([9]aneN_3)_2]^{3+} \quad (1)$$

$$d[M(N_4X)^{3+}]/dt = k_{obs}[Ni(N_4X)^{3+}] \quad (2)$$

$k_{obs} = k_1[Ni([9]aneN_3)_2^{2+}]$. The rate constants measured at 25.0 °C and the corresponding activation parameters are presented in Table 6. Under these conditions the reaction exhibits only a small acid dependence with an increase of ≈5–10% in the rate constants between 0.50 and 0.05 mol dm$^{-3}$ $H^+$ and no statistically significant change in value between 0.05 and 0.003 mol dm$^{-3}$ $H^+$. This dependence appears to be due to a medium effect, rather than to an acid–base equilibration, with the changes observed in the rate constant arising from a variation in the electrolyte cation from $H^+$ to $Li^+$.

In the presence of chloride ions the axial water molecule in $[Ni(N_4X)(OH_2)]^{3+}$ is equilibrated with the corresponding chloro complex and a more detailed mechanistic scheme is realized (Scheme 1). The electron-transfer rate constants for the reduction of $[Ni(N_4X)]^{3+}$ were observed to decrease with increasing chloride-ion concentration, owing to the lower reactivity of the $[Ni(N_4X)Cl]^{2+}$ species ($k_2$) (Fig. 5). However, the magnitude of the equilibrium constant, $K_{Cl}$, ensured that reaction of the chloro-substituted complex ion was the

$$\begin{array}{ccc} [Ni(N_4X)(OH_2)]^{3+} + [Ni([9]aneN_3)_2]^{2+} & \xrightarrow{k_1} & \\ K_{Cl} \Big\downarrow & & [Ni(N_4X)(OH_2)]^{2+} + [Ni([9]aneN_3)_2]^{3+} \\ [Ni(N_4X)Cl]^{2+} + [Ni([9]aneN_3)_2]^{2+} & \xrightarrow{k_2} & \end{array}$$

$$[Ni(N_4X)Cl]^{+} + [Ni([9]aneN_3)_2]^{3+}$$

$$\frac{d[M(N_4X)^{3+}]}{dt} = k_{obs}[Ni(N_4X)^{3+}]$$

$$k_{obs} = \frac{k_1 + k_2K_{Cl}[Cl^-]}{1 + K_{Cl}[Cl^-]}[Ni([9]aneN_3)_2^{2+}]$$

**Scheme 1**

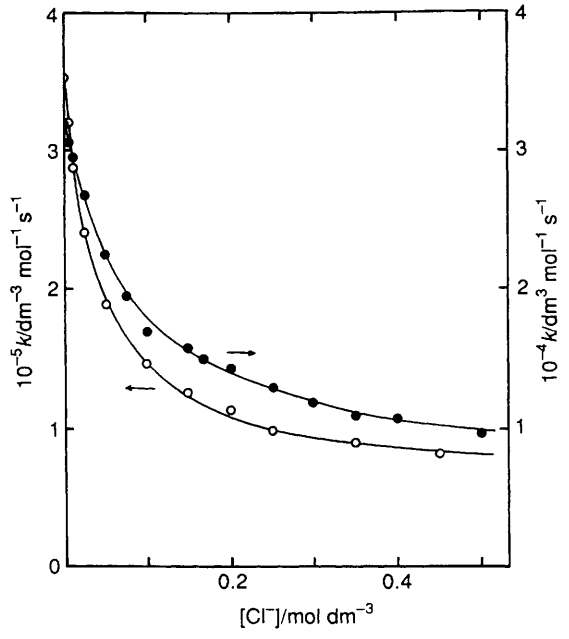


**Fig. 5** Variation of the second-order rate constant for the oxidation of $[Ni([9]aneN_3)_2]^{2+}$ by $[NiL^3(X)]^{n+}$ (●) and $[NiL^4(X)]^{n+}$ (○) in the presence of chloride ions (X = $H_2O$ or $Cl^-$)

dominant pathway under these conditions. For the $[NiL^3]^{3+}$ and $[NiL^4]^{3+}$ complexes the oxidation of $[Ni([9]aneN_3)_2]^{2+}$ was monophasic since the rate of chloride exchange is more rapid than the rate of electron transfer and the observed rate constants could be modelled using the expressions in Scheme 1. However, for $[NiL^1]^{3+}$, the rate of chloride exchange is comparable to that of electron transfer and at low chloride concentrations, in which there were appreciable amounts of both $[NiL^1(OH_2)]^{3+}$ and $[NiL^1(Cl)]^{2+}$, biphasic reactions were observed. In this range the observed data were fitted well by a double-exponential equation for concurrent reactions. The chloride binding constants $K_{Cl}$ and rate constants $k_2$ for the reduction of the $[Ni(N_4X)]^{3+}$ cations were calculated by means of a non-linear least-squares fit of the observed data by the complete expression for $k_{obs}$ and are presented in Table 6. The calculated equilibrium constant for $[NiL^1]^{3+}$ obtained from the electron-transfer kinetics matches closely the acid-independent equilibrium constant obtained from the rates of substitution [53] at the nickel(III) centre.

The self-exchange rate constants for both the aqua- and chloro-ligated complexes of $[NiL^1]^{3+}$, $[NiL^3]^{3+}$, and $[NiL^4]^{3+}$ obtained from a Marcus cross-correlation [54] are presented in Table 6. The values fall in the ranges (0.5–1.6) × $10^5$ and (1.3–2.8) × $10^4$ dm$^3$ mol$^{-1}$ s$^{-1}$ respectively. There appears to be a correspondence between the values obtained for each set of complexes. Those for the chloro-ligated species are similar to the 3.4 × $10^4$ and 1.4 × $10^5$ dm$^3$ mol$^{-1}$ s$^{-1}$ reported [27,55] for the self-exchange reactions of $[Ni(cyclam)Cl_2]^{+/0}$ and $[Ni(cyclam)(NO_3)_2]^{+/0}$. However, the increased self-exchange rate of the aqua complexes, both relative to the chloro species and to the corresponding $[Ni(cyclam)(OH_2)_2]^{3+/2+}$ reaction, is not readily explained.

The electron-transfer reaction with $[Ni(sar)]^{2+}$ (sar = 'sarcophagine', 3,6,10,13,16,19-hexaazabicyclo[6.6.6]icosane) could be examined only with the $[NiL^3]^{3+}$ cation since the remaining cations, with the much higher driving forces involved, yielded rates which were too fast for the stopped-flow apparatus, even at low temperatures. The temperature dependence for the observed rate constant yielded activation parameters of $\Delta H^{\ddagger}$ = 23.1 ± 3.0 kJ mol$^{-1}$ and $\Delta S^{\ddagger}$ = −54 ± 9 J K$^{-1}$ mol$^{-1}$ which are in accord with the values in Table 6. A similar dependence upon chloride concentration is also obtained and the observed and calculated rate constants

**Table 7** Chloride-ion dependence of the observed and calculated rate constants for the oxidation of $[Ni(sar)]^{2+}$ (2.93 × $10^{-4}$ mol dm$^{-3}$) by $[NiL^3]^{3+}$ (2.5 × $10^{-5}$ mol dm$^{-3}$) (25.0 °C, [H$^+$] = 0.50 mol dm$^{-3}$, $I$ = 1.0 mol dm$^{-3}$ $LiClO_4$)

| [Cl$^-$]/mol dm$^{-3}$ | $k_{obs}$/s$^{-1}$ | $10^{-5}$ $k$/ dm$^3$ mol$^{-1}$ s$^{-1}$ | $10^{-5}$ $k_{calc}$/ dm$^3$ mol$^{-1}$ s$^{-1}$ |
|---|---|---|---|
| 0.000 | 246 ± 7 | 8.41 ± 0.24 | 8.41 |
| 0.050 | 168 ± 6 | 5.74 ± 0.20 | 5.66 |
| 0.100 | 130 ± 2 | 4.44 ± 0.07 | 4.54 |
| 0.150 | 115 ± 5 | 3.93 ± 0.17 | 3.93 |
| 0.200 | 104 ± 3 | 3.56 ± 0.10 | 3.55 |
| 0.250 | 97.1 ± 1.1 | 3.32 ± 0.04 | 3.29 |
| 0.300 | 90.7 ± 1.0 | 3.10 ± 0.03 | 3.10 |
| 0.400 | 81.5 ± 1.3 | 2.79 ± 0.04 | 2.84 |
| 0.500 | 79.3 ± 2.2 | 2.71 ± 0.08 | 2.67 |

$k_2$ = (1.9 ± 0.1) × $10^5$ dm$^3$ mol$^{-1}$ s$^{-1}$, $K_{Cl}$ = 14 ± 1 mol dm$^{-3}$.

are presented in Table 7. The data yield a formation constant, $K_{Cl}$, of 14 ± 1 mol dm$^{-3}$ which is similar to the value obtained at 25 °C. The aqua and chloro rate constants are (8.60 ± 0.50) × $10^5$ and (1.9 ± 0.1) × $10^5$ dm$^3$ mol$^{-1}$ s$^{-1}$, respectively, leading to self-exchange values of 7.1 × $10^5$ and 2.0 × $10^5$ dm$^3$ mol$^{-1}$ s$^{-1}$, are about 13 and 14 times higher than the rates calculated from the reaction with $[Ni([9]aneN_3)_2]^{2+}$. It is of interest that both the outer-sphere reagents have self-exchange rates ≈6 × $10^3$ dm$^3$ mol$^{-1}$ s$^{-1}$ and appear to exhibit adiabaticity.[54] The cause of the much higher self-exchange rates in the complexes under consideration is not clear, neither is the apparent discrepancy in self-exchange values between the two reductants, especially since the formation constants for the complexes calculated from the kinetic data agree so well. Intuitively, on the basis of both charge delocalization and a decrease in the work terms accompanying the co-ordination of a chloride ion, a faster self-exchange rate for the $[Ni(N_4X)Cl]^{2+/+}$ couples would be anticipated. That this is not the case might be due to the structural rigidity of the ligand. Comparison of the co-ordination environment [14] for a number of metal complexes involving these hemicryptate ligands indicates that there is little variation in either bond lengths or angles resulting from changing the nature (or oxidation state) of the metal ion complexed. This would result in roughly similar inner-sphere reorganization energies ($\Delta G_{in}$) being obtained for the nickel–ligand interactions in each pair of complexes. The differences in the electron-transfer self-exchange rate then reflect a balance between the force constants and vibrational modes of the chloro and aqua species and the relative solvation of the two complexes. Clearly, in the absence of results from direct self-exchange experiments, further investigation into the structure and vibrational spectroscopy of these complexes is required to provide a better understanding of the calculated self-exchange rate constants.

## Acknowledgements

We thank the Natural Sciences and Engineering Research Council, Canada (NSERC) and the University of Victoria for their continued financial support of this research. In addition, we thank Mrs. K. Beveridge for her assistance with the crystal structures and Dr. N. F. Curtis for helpful discussions. Also, we thank NSERC (Canada) for the purchase of the DX-17MV stopped-flow spectrophotometer.

## References

1 L. F. Lindoy, *The Chemistry of Macrocyclic Ligand Complexes*, Cambridge University Press, New York, 1989.
2 A. Bianchi, M. Micheloni and P. Paoletti, *Coord. Chem. Rev.*, 1991, **110**, 17.

3 P. V. Bernhardt and G. A. Lawrance, *Coord. Chem. Rev.*, 1990, **104**, 297.
4 E. Kimura, X. Bu, M. Shionoya, S. Wada and S. Maruyama, *Inorg. Chem.*, 1992, **31**, 4542.
5 J.-M. Lehn, *Acc. Chem. Res.*, 1978, **11**, 49.
6 I. I. Creaser, R. J. Geue, J. M. Harrowfield, A. J. Herlt, A. M. Sargeson, M. R. Snow and J. Springborg, *J. Am. Chem. Soc.*, 1982, **104**, 6016; I. I. Creaser, J. M. Harrowfield, A. J. Herlt, A. M. Sargeson, J. Springborg, R. J. Geue and M. R. Snow, *J. Am. Chem. Soc.*, 1977, **99**, 3181.
7 B. Dietrich, J.-M. Lehn and J. P. Sauvage, *Chem. Commun.*, 1970, 1055; B. Dietrich, J.-M. Lehn, J. P. Sauvage and J. Blanzat, *Tetrahedron*, 1973, **29**, 1629.
8 J. C. A. Boeyens and S. M. Dobson, *Stereochemistry of Organometallic and Inorganic Compounds*, Elsevier, Amsterdam, 1987, vol. 2, p. 1.
9 R. D. Gandour and T. M. Fyles, *J. Incl. Phen. Mol. Rec. Chem.*, 1992, **12**, 313.
10 K. Henrick, P. A. Tasker and L. F. Lindoy, *Prog. Inorg. Chem.*, 1985, **33**, 1.
11 J. P. Ounsworth and L. Weiler, *J. Chem. Educ.*, 1987, **64**, 568.
12 D. G. Fortier, Ph.D. Dissertation, University of Victoria, 1989; C. Xu, Ph.D. Dissertation, University of Victoria, 1991.
13 (*a*) D. G. Fortier and A. McAuley, *Inorg. Chem.*, 1989, **28**, 655; (*b*) D. G. Fortier and A. McAuley, *J. Am. Chem. Soc.*, 1990, **112**, 2640; (*c*) K. Beveridge, A. McAuley and C. Xu, *Inorg. Chem.*, 1991, **30**, 2074.
14 N. F. Curtis, *Coord. Chem. Rev.*, 1968, **3**, 3.
15 G. A. Melson (Editor), *Coordination Chemistry of Macrocyclic Compounds*, Plenum, New York, 1979.
16 D. C. Olson and J. Vasilevski, *Inorg. Chem.*, 1969, **8**, 1611; 1971, **10**, 463.
17 D. H. Busch, *Adv. Chem. Ser.*, 1971, **100**, 44; *Acc. Chem. Res.*, 1978, **11**, 3.
18 R. I. Haines and A. McAuley, *Coord. Chem. Rev.*, 1981, **33**, 77.
19 K. Nag and A. Chakravorty, *Coord. Chem. Rev.*, 1980, **32**, 87.
20 E. Zeigerson, G. Ginsburg, N. Schwartz, Z. Luz and D. Meyerstein, *J. Chem. Soc., Chem. Commun.*, 1979, 241.
21 L. Fabbrizzi, *J. Chem. Soc., Chem. Commun.*, 1979, 1063.
22 A. G. Lappin and A. McAuley, *Adv. Inorg. Chem.*, 1988, **32**, 241.
23 E. S. Gore and D. H. Busch, *Inorg. Chem.*, 1973, **12**, 1.
24 R. I. Haines and A. McAuley, *Inorg. Chem.*, 1980, **19**, 719.
25 K. Weighardt, W. Schmidt, W. Herrmann and H. J. Kuppers, *Inorg. Chem.*, 1983, **22**, 2953.
26 P. Chaudhuri and K. Wieghardt, *Prog. Inorg. Chem.*, 1987, **35**, 329.
27 A. McAuley, P. R. Norman and O. Olubuyide, *Inorg. Chem.*, 1984, **23**, 1939; *J. Chem. Soc., Dalton Trans.*, 1984, 1501.
28 HEADSTART VO.1, Princeton Applied Research, Princeton, NJ, 1985.
29 K. J. Ellis and A. McAuley, *J. Chem. Soc., Dalton Trans.*, 1973, 1533.
30 (*a*) P. Coppens, L. Lieserowitz and D. Rabinovich (modified by G. W. Bushnell), Correction of Crystallographic Data for Absorption and Secondary Extinction Effects, University of British Columbia, 1969; (*b*) L. Y. Le Page, E. J. Gabe and P. S. White, EMPABS, Nonius Computer Program, National Research Council, Ottawa, 1986.
31 G. M. Sheldrick, SHELX 76, Program for Crystal Structure Determinations, Cambridge University, Cambridge, 1976.
32 P. Main, L. Lessinger, M. M. Woolfson, G. Germain and J. P. Declarecq, MULTAN 77, Universities of York and Louvain, 1977.
33 *International Tables for X-Ray Crystallography*, Kynoch Press, Birmingham, 1974, vol. 4.
34 E. K. Barefield, F. Wagner, A. W. Herlinger and A. R. Dahl, *Inorg. Synth.*, 1975, **16**, 220.
35 C. K. Johnson, ORTEP, Report ORNL-5138, Oak Ridge National Laboratory, Oak Ridge, TN, 1976.
36 B. Bosnich, C.-K. Poon and M. L. Tobe, *Inorg. Chem.*, 1965, **4**, 1102.
37 L. Y. Martin, L. J. De Hayes, L. J. Zompa and D. H. Busch, *J. Am. Chem. Soc.*, 1974, **96**, 4047.
38 G. J. McDougall, R. D. Hancock and J. C. A. Boeyens, *J. Chem. Soc., Dalton Trans.*, 1978, 1438.
39 T. N. Margulis and L. J. Zompa, *Inorg. Chim. Acta*, 1978, **28**, L157.
40 S. M. Hart, J. C. A. Boeyens, J. P. Michael and R. D. Hancock, *J. Chem. Soc., Dalton Trans.*, 1983, 1601.
41 J. C. A. Boeyens, R. D. Hancock and V. J. Thöm, *J. Crystallogr. Spectrosc. Res.*, 1984, **14**, 261.
42 I. S. Crick, R. W. Gable, B. F. Hoskins and P. A. Tregloan, *Inorg. Chim. Acta*, 1986, **111**, 35.
43 T. W. Hambley, *J. Chem. Soc., Dalton Trans.*, 1986, 565.
44 N. W. Alcock, N. Herron and P. Moore, *J. Chem. Soc., Dalton Trans.*, 1978, 1282.
45 V. J. Thöm, C. C. Fox, J. C. A. Boeyens and R. D. Hancock, *J. Am. Chem. Soc.*, 1984, **106**, 5947.
46 P. R. Louis, Y. Agnus and R. Weiss, *Acta Crystallogr., Sect. B*, 1979, **35**, 2905; P. R. Louis, B. Metz and R. Weiss, *Acta Crystallogr., Sect. B*, 1974, **30**, 774.
47 A. Abragam and B. Bleaney, *Electron Paramagnetic Resonance of Transition Ions*, Clarendon Press, Oxford, 1970; P. W. Atkins and M. C. R. Symons, *The Structure of Inorganic Radicals*, Elsevier, New York, 1967.
48 F. V. Lovecchio, E. S. Gore and D. H. Busch, *J. Am. Chem. Soc.*, 1974, **96**, 3109.
49 I. I. Creaser, L. M. Engelhardt, J. M. Harrowfield, E. R. Krausz, G. M. Moran, A. M. Sargeson and A. H. White, *Aust. J. Chem.*, 1993, **46**, 111.
50 R. Yang and L. J. Zompa, *Inorg. Chem.*, 1976, **15**, 1499.
51 W. E. Geiger, *Prog. Inorg. Chem.*, 1985, **33**, 275.
52 M. G. Fairbank and A. McAuley, *Inorg. Chem.*, 1985, **24**, 1233.
53 C. Xu, T. W. Whitcombe and A. McAuley, unpublished work.
54 R. A. Marcus, *Annu. Rev. Phys. Chem.*, 1964, **15**, 155; N. Sutin, *Prog. Inorg. Chem.*, 1983, **30**, 441.
55 A. McAuley, T. Palmer and T. W. Whitcombe, *Can. J. Chem.*, 1993, **73**, 1792.


*Received* 14*th February* 1994; *Paper* 4/00902I